

Diagnosis of Different Types of Air-Gap Eccentricity Fault in Switched Reluctance Motors Using Transient Finite Element Method

H. Nazari ^{1,*} and N. Rostami ²

¹Department of Electrical Engineering, Ahar Branch, Islamic Azad University, Ahar, Iran

²Faculty of Electrical and Computer Engineering, University of Tabriz, Tabriz, Iran

ABSTRACT

This paper presents a method for diagnosis of eccentricity fault in a switched-reluctance motor (SRM) during offline and standstill modes. In this method, the fault signature is differential induced voltage (DIV) achieved by injecting diagnostic pulses to the motor windings. It will be demonstrated by means of results that there is a correlation between differential induced voltage and eccentricity occurrence. The method employs three-dimensional transient finite-element method (TFEM) analysis to calculate differential induced voltage in three phase 6/4 SRM. In this method, first of all the fault presence is distinguished. Next, an algorithm is presented for the detection of fault location or faulty phase. Then, the direction of fault is recognized by a simple comparative technique, and finally, results comparing is proposed to detect fault type.

KEYWORDS: Eccentricity fault, Differential induced voltage, Transient finite-element method.

1. INTRODUCTION

Switched reluctance motor (SRM) have been a good and proper choice for industrial applications such as hybrid electric vehicle, air compressor, fuel pumps, aerospace applications, renewable energy harvesting and home appliances due to its advantages like simplicity in winding and manufacturing, durability, rotor permissible temperature, high efficiency, operating in adjustable speed ranges and relatively easy speed control circuitry [1-3].

Faults and failures of critical electromechanical parts can indeed lead to excessive downtimes and cause many costs in maintenance and lost operation. Therefore, it is important to detect faulty conditions and solve them before occurrence of significant damages on the motor.

One of the most common faults that may occur in the motor is air-gap eccentricity. Airgap eccentricity is divided into three eccentricity types named by static eccentricity (SE), dynamic eccentricity (DE), and mixed eccentricity (ME) [4]. Eccentricity fault causes an unbalanced magnetic pull which results in vibration, acoustic noise, rotor deflection and bearing wear. This increases the risk of stator and rotor rub, which can cause serious damage in the motor stator or rotor core [5]. Several contributions can be found in the literature dealing with the performance analysis of electrical machines under eccentricity conditions.

Recently, several studies have concentrated their interest to diagnosis of various faults in electrical machines to avoid unexpected loss. In [1] effect of mixed eccentricity on flux-linkages has been studied using FE analysis. The obtained results show that motor with 10%, 20% and 40% mixed eccentricity has 4.5%, 13.5% and 22.5% maximum increase in flux linkage as well as inductance of faulty phase. Furthermore, the flux linkage values of the healthy

phase obtained for eccentric motor with 10% to 40% eccentricity are 3.5% up to 15.2% higher.

The method used in [4] is based on the spectral analysis of the complex apparent power modulus for detecting the occurrence of mixed airgap eccentricity in operating three-phase induction motors. This method is constructed based on the behavior of spectral component at frequency of $f_r = f(1 - s)/p$ and provides simultaneous information about the current and voltage.

In [6] eccentricity diagnosis method has been constructed upon the produced current signature (PCS) analysis of the motor phases. It has been depicted that when eccentricity percentage changes from 10% to 20%, 30%, 40% and 50% eccentricity severity factor (ESF) increases from 1.1 p.u to 1.2, 1.35, 1.55 and 1.85 p.u.

According to [7] by changing eccentricity percentage up to 60% the stator voltage varies in range of 21%-23% in faulty phase and in the range of 7%-10% in healthy phases.

Faiz *et al.* [8] have shown that voltage induced in a particular idle phase of an SRM is a suitable criterion for diagnosis of eccentricity. Based on the proposed approach if the faulty phase is excited, the induced voltage in the phase adjacent to the faulty phase considerably increases as the percentage of the eccentricity increases.

Reference [9] illustrates that torque characteristic variations in consequence of eccentricity are not evident at the rated current. But at low current, eccentricity, even in the order of 30%, can considerably affect the motor torque. It is found that when eccentricity degree increases, the fundamental harmonic of the static torque profile increases. In addition, 3rd harmonic varies in a wide range when eccentricity degree is between 10% and 30%. Losses could be used to detect eccentricity.

In [10] all kinds of important losses in SRM including of ohmic losses and iron losses (consist of hysteresis and eddy-current losses) are studied to diagnosis eccentricity. It was shown that the flux linkages waveforms and all kinds of losses in SRM increase when the amount of eccentricity percentage become more. With comparing between DE and SE it is seen that SE has more

visible effect on losses. Radial force has been investigated as an index to detect eccentricity fault.

Computed results in [11] show that the radial force has increased by a factor of 6 when the eccentricity has changed from 10% to 50%.

Simulation results in [13] indicate that both methods of wavelet transform and Gyration radius of the stator current signal could detect eccentricity fault in an induction motor. It has been shown that with increasing eccentricity degree the energy of the nodes and radius of phase space diagram increase simultaneously.

This paper presents a method to detect eccentricity fault presence, fault location, fault direction and fault types based on differential induced voltage signature using 3-D transient finite element method. The FE software used in this study is Maxwell 15.0.

2. ECCENTRICITY FAULT

As mentioned in previous section eccentricity fault is divided into three types named by SE, SE and ME. According to Fig.1, in static eccentricity minimum air-gap location is fixed in front of faulty phase when rotor revolves. It means that rotor symmetry center (r) and rotation symmetry center (ω) are exactly the same but both different with the stator symmetry center (s). SE fault reason could be astator core elliptical shape, rotor imprecise location

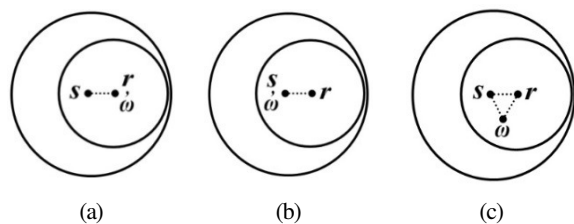


Fig. 1. Rotor, stator and rotation positions and their symmetry centers in eccentric modes: (a) SE, (b) DE and (c) ME

and burden of rotor or load. In dynamic eccentricity, the minimum air-gap revolves with rotation of rotor. It means that the location of fault is different in two arbitrary moments. DE happens in result of rotor bent shaft, bearing erosion, mechanical stresses and asymmetric thermal expansion of the rotor in critical speeds. In actual machinery both SE and DE have an intensive trend to coexist called mixed eccentricity (ME). The reason for ME could be worn

bearings [6, 7]. These three types of eccentricity have been illustrated in Fig. 1. It is important to say that all kinds of eccentricity fault are usual in motor up to 10% because of manufacturing process. The degree of mixed eccentricity is defined as:

$$\varepsilon = \left(\frac{m}{g}\right) \times 100 (\%) \quad (1)$$

Where ε is the degree of eccentricity, g is the normal air gap in healthy motor and m is transfer vector as follow:

$$m = \begin{cases} s.\omega & \text{for, SE} \\ \omega.r & \text{for, DE} \\ s.r & \text{for, ME} \end{cases} \quad (2)$$

In Eq. (2), $s.\omega$, $\omega.r$ and $s.r$ are called static, dynamic and mixed transfer vectors, respectively.

3. REFERENCE MOTOR PARAMETERS AND SPECIFICATIONS

As illustrated in Fig.2, the proposed motor is a three phase 6/4 SRM. The motor phases are named in counterclockwise. Motor analysis is done at steady state, offline and standstill modes. In other words, there is no rotation for motor in proposed method. All details, parameters and motor specifications used in this motor, like material and motor dimension have been reported in Table 1. As stated before, the stator and rotor material is steel M19 that is one of the most used materials in the motors. Table 2 includes the values of B-H curve for steel M19 and Fig. 3 shows the B-H curve.

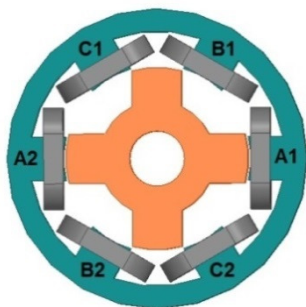


Fig. 2. Proposed three phase 6/4 SRM.

4. ANALYTICAL THEORY

In the proposed method, motor is in standstill and offline mode. When one phase is excited in the SRM, the major section of the produced flux flows in the excited phase. But, a small section of the flux, called mutual flux, flows in other phase windings.

Table 1. Reference Motor Parameters

Parameter	Value(mm)
Stator outer diameter	120
Stator inner diameter	75
Stator core length	35
Stator core thickness	9
Stator pole length	13.84
Stator pole arc	30°
Stator pole number	6
No. of turns per coil	80
Rotor outer diameter	73
Rotor inner diameter	30
Air-gap length	1
Rotor core thickness	10
Rotor pole length	12.4
Rotor pole arc	36°
Rotor pole number	4
Material	M19

Table 2. M19 B-H Curve Values

B (tesla)	H (A/m)	B (tesla)	H (A/m)
0	0	1.549	1815.58
0.414	16.52	1.574	2286.02
0.633	31.55	1.603	2874.08
0.894	63.1	1.636	3609.16
1.039	95.43	1.673	4528
1.149	135.84	1.714	5676.56
1.232	186.36	1.759	7112.25
1.297	249.5	1.807	8906.87
1.348	328.43	1.856	11150.14
1.389	427.09	1.903	13954.22
1.424	550.41	1.947	17459.33
1.453	704.57	1.986	21840.72
1.478	897.26	2.014	27317.45
1.502	1138.13	2.031	34163.37
1.525	1439.22	2.036	37579.71

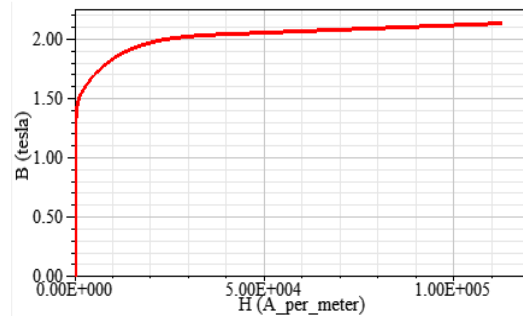


Fig. 3. M19 B-H curve

The reason for presence of mutual flux in SRM is leakage flux created between the energized phase and other phases [8]. First, assume that phase A is a fully aligned position as faulty phase and two out-of-phase pulses (i.e., 180° difference) with amplitude of $5V_{pp}$ and frequency of 1KHz are injected into both coils of phase A (coil A1 and coil A2) as shown in Fig.4. The induced voltage is as below

$$v_{L,A1} = L_{A1} \frac{di_{A1}}{dt} + L_{A1,A2} \frac{di_{A2}}{dt} \quad (3)$$

$$v_{L,A2} = L_{A2} \frac{di_{A2}}{dt} + L_{A1,A2} \frac{di_{A1}}{dt}$$

where $v_{L,A1}$, L_{A1} , i_{A1} , $L_{A1,A2}$, i_{A2} , $v_{L,A2}$, L_{A2} , $L_{A2,A1}$ are induced voltage of coil A1, self-inductance of coil A1, current of coil A1, mutual inductance between coil A1 and coil A2, current of coil A2, induced voltage of coil A2, self-inductance of coil A2 and mutual inductance between coil A1 and coil A2, respectively. It is observed from Eq. (3) that $v_{L,A1}$ is proportional to L_{A1} , di_{A1}/dt , $L_{A1,A2}$ and di_{A2}/dt . Also, $v_{L,A2}$ is proportional to L_{A2} , di_{A2}/dt , $L_{A1,A2}$ and di_{A1}/dt . Values of L_{A1} , L_{A2} and $L_{A1,A2}$ in Eq. (3) are constant, because there is no rotation of rotor. So, the Eq. (3) changes to:

$$\begin{aligned} v_{L,A1} &= A \frac{di_{A1}}{dt} + B \frac{di_{A2}}{dt} \\ v_{L,A2} &= C \frac{di_{A2}}{dt} + B \frac{di_{A1}}{dt} \end{aligned} \quad (4)$$

Where A , B and C are constant.

Differential induced voltage is the difference between induced voltages of two coils in one phase. For example, ΔV_A , ΔV_B and ΔV_C stand for differential induced voltage related to the phase A , B and C , respectively, as follow:

$$\Delta V_k = v_{k2} - v_{k1} \quad (5)$$

where, ΔV_k , v_{k2} and v_{k1} are the differential induced voltage of phase k , induced voltage of coil $k2$, induced voltage of coil $k1$ and phase k , respectively.

With substituting Eq. 4 in Eq. 5 for phase A:

$$\begin{aligned} \Delta V_A &= (C \frac{di_{A2}}{dt} + B \frac{di_{A1}}{dt}) - (A \frac{di_{A1}}{dt} + B \frac{di_{A2}}{dt}) \\ \Delta V_A &= (C - B) \frac{di_{A2}}{dt} - (A - B) \frac{di_{A1}}{dt} \end{aligned} \quad (6)$$

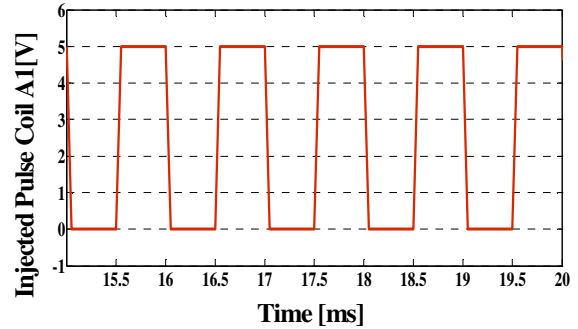
Where $A - B$ and $C - B$ are constant. To simplify the Eq. (6) suppose:

$$\begin{aligned} C - B &= K1 \\ A - B &= K2 \end{aligned} \quad (7)$$

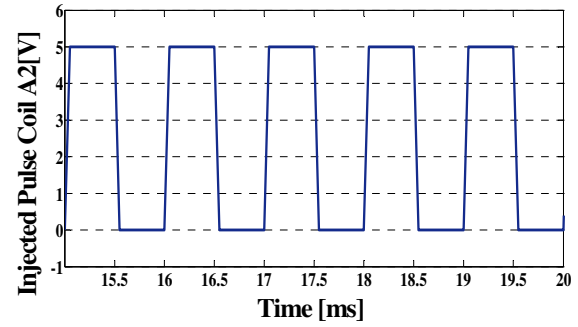
Where $K1$ and $K2$ are constant. So Eq. (6) changes as below with substituting Eq. (7):

$$\Delta V_A = K1 \frac{di_{A2}}{dt} - K2 \frac{di_{A1}}{dt} \quad (8)$$

Eq. (8) shows that differential induced voltage in phase A is proportional to slope of induced current in coil A1 and coil A2 (di_{A1}/dt and di_{A2}/dt).



(a)



(b)

Fig. 4. Injected pulse to phase A (a) coil A1 (b) coil A2

Now, it is turn to apply eccentricity to the motor from 20% to 60%. First, two out-of-phase pulses as shown in Fig. 4 are applied to the phase A.

Resulted currents in coil A1 and coil A2 have been shown in Fig. 5. Slope of current related to the coil A1 decreases but slope of current in coil A2 increases when eccentricity severity increases from zero (healthy motor) up to 60% as shown in Fig.5. In other words, in Eq. (8) the first term (di_{A2}/dt) increases and second term (di_{A1}/dt) decreases. So, the total value of Eq. (8) increases with increasing fault severity. It can be concluded that differential induced voltage has a high and significant sensitivity to the eccentricity fault severity and is a proper criterion to detect fault presence, fault location, fault direction and fault type. In next section, the simulation results configures the theoretical analysis.

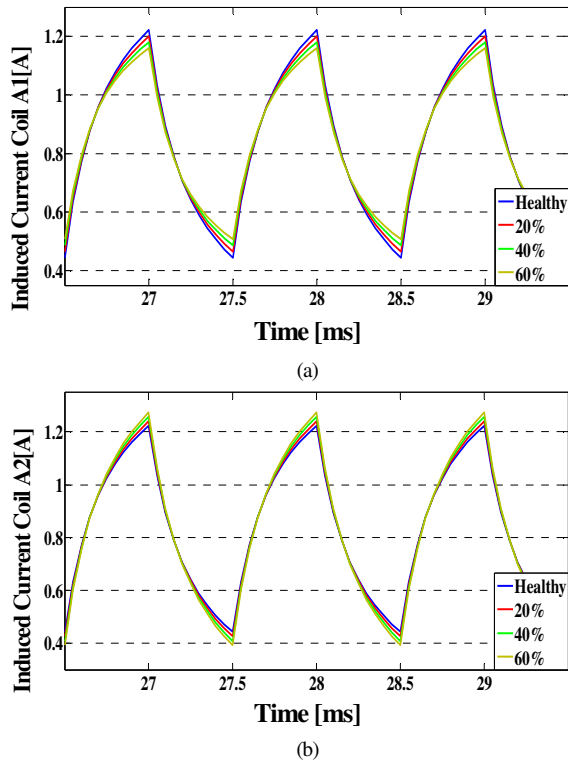


Fig. 5. Induced current in phase A with different degrees of eccentricity when phase A is in fully aligned position and is excited (a) coil A1 (b) coil A2

5. PROPOSED METHOD AND SIMULATION RESULTS

First, phase A is in a fully aligned position and two aforementioned out-of-phase pulses are injected into both coils of phase A (coil A1 and coil A2). So an induced voltage will produce in all coils of all phases. Resulted differential induced voltage with eccentricity severity of 0%, 20%, 40% and 60% in all phases are shown in Fig.6. It is clear that in healthy motor, differential induced voltage in all phases are almost zero. Next, phase B is in fully aligned position and phase A is excited again and differential induced voltage is computed. Then, phase C is in fully aligned position while phase A is energized once again and differential induced voltage is obtained. This method is repeated when phase B and C are energized and phase A, B and C are in fully aligned position, respectively. These jobs could be summarized in three steps as follows:

- Phase A is excited when phase A, B and C are in fully aligned position, respectively.
- Phase B is excited when phase A, B and C are in fully aligned position, respectively.

- Phase C is excited when phase A, B and C are in fully aligned position, respectively.

Resulted differential induced voltages are illustrated in Fig.6 for healthy and faulty motor and are reported in details in Table 3 for motor with 60% eccentric condition.

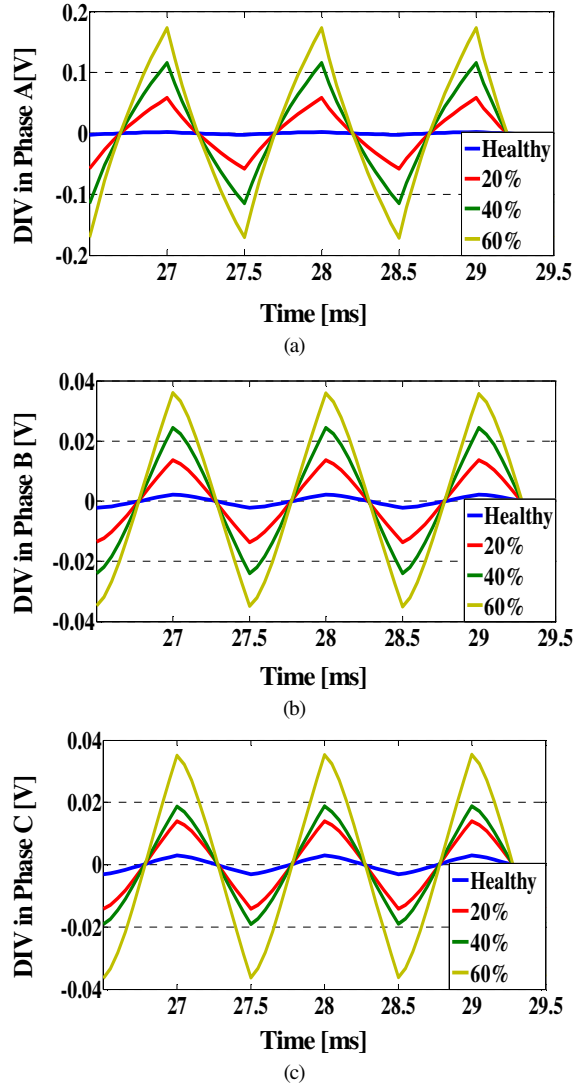


Fig. 6. Differential induced voltage in phase windings, when phase A is in fully aligned position and is excited: (a) phase A, (b) phase B, (c) phase C.

As illustrated in Fig. 6, in healthy motor the differential induced voltage is zero because, the induced voltage in coil A1 and coil A2 is equal. When eccentricity increases from zero to 20%, 40% and 60% differential induced voltage increases in a manner in all phases.

Table 3. Differential induced voltage for phase windings in 60% eccentricity (mv)

Excited Phase	Sampled Phase	Alignment Phase		
		A	B	C
A	A	173	194	194
	B	36	16	7
	C	36	7	16
B	A	36	57	57
	B	138	84	3
	C	36	10	18
C	A	36	57	57
	B	36	18	10
	C	120	3	84

In phase A as faulty phase when eccentricity increases from zero to 20%, 40% and 60% differential induced voltage increases from 2.2mv to 58mv, 115mv and 173mv, respectively. In phase B with the same eccentricity values the differential induced voltage increases from 2.2mv to 13.7mv, 24.4mv to 36mv, respectively. In phase C with the same eccentricity values the differential induced voltage increases from 3.1mv to 14mv, 18.8mv and 35.5mv, respectively. This results show that differential induced voltage has a high sensitivity to eccentricity severity so it is a good and proper criterion to detect airgap eccentricity fault. Now, it is turn to define differential induced voltage matrix (DIVM) and minor differential induced voltage matrix (MDIVM) to use to detect fault presence, fault location, fault direction and fault type in next section. Assume that phase A is excited; therefore, DIVM and MDIVM are defined as follows:

$$\text{DIVM} = \begin{bmatrix} \Delta_{aa} & \Delta_{ab} & \Delta_{ac} \\ \Delta_{ba} & \Delta_{bb} & \Delta_{bc} \\ \Delta_{ca} & \Delta_{cb} & \Delta_{cc} \end{bmatrix} \quad (9)$$

$$\text{MDIVM}(\Delta_{aa}) = \begin{bmatrix} \Delta_{bb} & \Delta_{bc} \\ \Delta_{cb} & \Delta_{cc} \end{bmatrix} \quad (10)$$

$$\text{MDIVM}(\Delta_{bb}) = \begin{bmatrix} \Delta_{aa} & \Delta_{ac} \\ \Delta_{ca} & \Delta_{cc} \end{bmatrix} \quad (11)$$

$$\text{MDIVM}(\Delta_{cc}) = \begin{bmatrix} \Delta_{aa} & \Delta_{ab} \\ \Delta_{ba} & \Delta_{bb} \end{bmatrix} \quad (12)$$

where matrix rows show fully aligned phases, and columns depict the sampled phases. For instance, Δ_{ab} shows the differential induced voltage in two coils of phase B when phase A is in the fully

aligned position. These matrixes are used to complete the proposed method in next section.

6. AIRGAP ECCENTRICITY FAULT DETECTION STRATEGY

This section is going to analyze the fault details by means of DIVM and MDIVM. Fault details include fault presence, fault location, fault direction and fault type.

6.1. Fault Presence Diagnosis (FPD)

As stated before, differential induced voltage between two coils in one phase in healthy motor is almost zero for all motor phases. So, the eccentricity causes a changes in magnitude of induced voltage of motor phases. In fact, a difference between Induced voltage magnitudes of two coils of all phases will be produced. This difference can be used to detect the occurrence of fault. Therefore, fault presence is achieved by following the changes of differential induced voltage in the coil windings.

6.2. Fault location Diagnosis (FLD)

First, we are going to compute the DIVM and MDIVM to detect fault location. By using Table 3 and Eqs. (9)-(12) we have:

$$\text{DIVM} = \begin{bmatrix} 173 & 36 & 36 \\ 194 & 16 & 7 \\ 194 & 7 & 16 \end{bmatrix} \quad (13)$$

$$\text{MDIVM}(\Delta_{aa}) = \begin{bmatrix} 16 & 7 \\ 7 & 16 \end{bmatrix} \quad (14)$$

$$\text{MDIVM}(\Delta_{bb}) = \begin{bmatrix} 173 & 36 \\ 194 & 16 \end{bmatrix} \quad (15)$$

$$\text{MDIVM}(\Delta_{cc}) = \begin{bmatrix} 173 & 36 \\ 194 & 16 \end{bmatrix} \quad (16)$$

It is seen from Eqs. (13)-(16) that only MDIVM (Δ_{aa}) related to the phase A is symmetric while MDIVM (Δ_{bb}) and MDIVM (Δ_{cc}) related to the phase B and C, respectively, are asymmetric; therefore it can be deduced that MDIVM for faulty phase is symmetric and for healthy phases are asymmetric and equal. In other words, when a symmetric MDIVM and two unequal asymmetric MDIVM are observed, the faulty phase and healthy one could be detected easily.

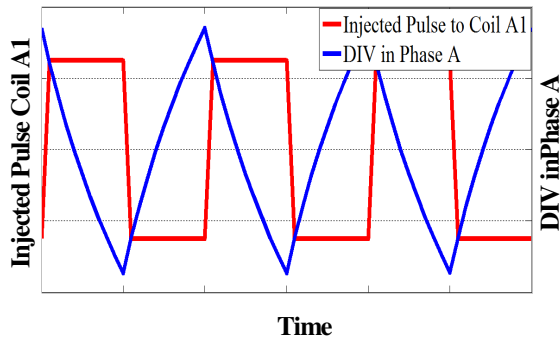


Fig. 7. Comparison differential induced voltage with injected pulse to coil A1

6.3. Fault Direction diagnosis (FDD)

In this part a method for fault direction detection in faulty phase is discussed meaning fault has occurred in coil 1 or coil 2 of faulty phase. For this purpose, it is necessary to compare the differential induced voltage and injected pulse to the windings. Here, the differential induced voltage in phase A [Fig.6 (a)] and one of two injected pulses to phase A [Fig.4] in 60% eccentric are chosen to compare as illustrated in Fig.7. In this figure the charging time of injected pulse to coil A1 and differential induced voltage phase A is different meaning they are out of phase (i.e., 180° difference). In this condition, the air-gap length has decreased in front of pole A1. In other words, fault has occurred toward coil A1. If input pulse coil A1 and differential induced voltage are in phase, i.e., their charging and discharging time is the same, fault has occurred toward coil A2. It means that air-gap length decreases in front of coil A2.

6.4. Fault Type Diagnosis (FTD)

In previous sections, fault presence, fault location and fault direction were discussed. Now, it is turn to detect fault type using the proposed method. As mentioned before, in SE minimum airgap is fixed in front of faulty phase i.e., fault location does not rotate with rotor rotation; therefore, the results are exactly the same in Table 3. So, according to Eqs. (13)-(16) in SE, MDIVM of faulty phase is symmetric and is asymmetric and equal for two healthy phases. In DE minimum air-gap revolves with rotor rotation i.e., the fault location is in specific phase in any moment. It means when phase A is in fully alignment and phase A, B and C are injected,

the results are the same when phase B is in fully alignment and phase A, B and C are injected as follows:

$$\text{DIVM} = \begin{bmatrix} 173 & 194 & 194 \\ 194 & 173 & 194 \\ 194 & 194 & 173 \end{bmatrix} \quad (17)$$

$$\begin{aligned} \text{MDIVM}(\Delta_{aa}) &= \text{MDIVM}(\Delta_{bb}) \\ &= \text{MDIVM}(\Delta_{cc}) \end{aligned}$$

$$= \begin{bmatrix} 173 & 194 \\ 194 & 173 \end{bmatrix}. \quad (18)$$

It is observed from Eq. (18) that in DE the minor matrix for all phases are symmetric and equal. So the DE is also detected easily by the proposed method.

If MDIVMs of all phases have no specific manner and are asymmetric and unequal, the ME has happened. In other words, if MDIVMs are not similar to those in SE and DE, then ME has occurred. Therefore, in this section with a simple comparison, fault type distinguished.

Generally, it can be said that using the proposed method fault presence, fault location, fault direction and fault type could be detected easily. The main advantages of this method are:

- Proposed method has no effect on normal operation of SRM.
- Proposed method is a sensorless method that simplifies the structure of method in practical applications.
- Proposed method is comprehensive method to detect fault details including fault presence, fault location, fault direction and fault type.

6. CONCLUSION

In this paper, an offline and standstill method was proposed to detect airgap eccentricity fault in a 6/4 SRM. Proposed method was done through 3D-TFEM using Maxwell-15.0 package. In section 2 the eccentricity fault and its different types have been discussed. Then, in section 3 motor parameters, specifications and materials have been presented. Section 4 includes analytical theory. In this section two out-of-phase pulses are injected to motor windings then, resulted differential induced voltage are used as fault detection signature to diagnosis air-gap eccentricity fault details. By investigating of

resulted differential induced voltage it is observed that differential induced voltage has a high sensitivity to occurrence of eccentricity fault. Next, in section 5 fault details detection has been presented. Fault presence diagnosis can be done easily by comparison of magnitude of DIV in healthy and faulty conditions. Fault location and fault type can be detected through differential induced voltage matrix and minor differential induced voltage matrix. Finally, fault direction diagnosis is possible using a simple comparison between DIV in one phase and injected pulse to one of its coils. So, it can be concluded that differential induced voltage is a good and proper criterion to detect fault presence, fault location, fault direction and fault type.

REFERENCES

- [1] E. Afjei and H. Torkaman, "Airgap eccentricity fault diagnosis in switched reluctance motor," *Proc. of the IEEE 1st Power Electronic, Drive Systems and Technologies Conference*, pp. 290-294, 2010.
- [2] M.R. Tavakoli, H. Torkaman and E. Afjei, "Eccentricity faults compensation in SRMs by counterbalancing ampere turns in facing poles," *Proc. of the IEEE 4th Power Electronic, Drive Systems and Technologies Conference*, pp. 66-71, 2013.
- [3] H. Torkaman, E. Afjei and H. Amiri, "Static eccentricity fault diagnosis in switched reluctance motor" *Proc. of the IEEE International Conference on Power and Energy*, pp. 218-221, 2010.
- [4] M. Drif and A.J.M Cardoso, "Airgap eccentricity fault diagnosis, in three-phase induction motors, by the complex apparent power signature analysis," *Proc. of the IEEE International Symposium on Power Electronics, Electrical Drives, Automation and Motion*, pp. 61-65, 2006.
- [5] J. Hong, S.B. Lee, Ch. Kral and A. Haumer, "Detection of airgap eccentricity for permanent magnet synchronous motors based on the d-Axis inductance," *IEEE Transactions on Power Electronics*, vol. 27, no. 5, pp. 378-384, 2012.
- [6] H. Torkaman, E. Afjei and P. Yadegari, "Static, dynamic, and mixed eccentricity faults diagnosis switched reluctance motors using transient finite element method and experiments," *IEEE Transactions on Magnetics*, vol. 48, no. 8, pp. 2254-2264, 2012.
- [7] H. Torkaman and E. Afjei, "Sensorless method for eccentricity fault monitoring and diagnosis in switched reluctance machines based on stator voltage signature," *IEEE Transactions on Magnetics*, vol. 49, no. 2, pp. 912-920, 2013.
- [8] J. Faiz and S. Pakdelian, "Diagnosis of static eccentricity in switched reluctance motors based on mutually induced voltages," *IEEE Transactions on Magnetics*, vol. 44, no.8 pp. 2029-2034, 2008.
- [9] J. Faiz and S. Pakdelian, "Finite element analysis of switched reluctance motor under dynamic eccentricity fault," *Proc. of the IEEE 12th International Power Electronics and Motion Control Conference*, pp.1042-1046, 2006.
- [10] R. Moradi, E. Afjei, H. Torkaman, A. Hajihosseini, "Investigation of power losses in switched reluctance motors due to rotor eccentricity utilizing FEM," *Proc. of the IEEE 4th Power Electronics, Drive Systems and Technologies Conference*, pp. 78-82, 2013.
- [11] H. Torkaman, "Rotor fault analysis and diagnosis in three-phase outer-rotor switched reluctance motor," *Proc. of the IEEE 4th Power Electronics, Drive Systems and Technologies Conference*, pp. 93-96, 2013.
- [12] M. Ahmadi, J. Poshtan and M. Poshtan, "Static eccentricity fault detection in induction motors using Wavelet Packet decomposition and Gyration radius" *Proc. of the IEEE 1st International Conference on Communications, Signal Processing and their Applications*, pp. 1-5, 2013.